The Dynamics of Transition to Turbulence in Plane Couette Flow

D. Viswanath

Department of Mathematics, University of Michigan, 530 Church Street, Ann Arbor, MI 48109, USA, divakar@umich.edu

Summary. In plane Couette flow, the incompressible fluid between two plane parallel walls is driven by the motion of those walls. The laminar solution, in which the streamwise velocity varies linearly in the wall-normal direction, is known to be linearly stable at all Reynolds numbers (Re). Yet, in both experiments and computations, turbulence is observed for $Re \gtrsim 360$.

In this article, we show that for certain *threshold* perturbations of the laminar flow, the flow approaches either steady or traveling wave solutions. These solutions exhibit some aspects of turbulence but are not fully turbulent even at $Re = 4{,}000$. However, these solutions are linearly unstable and flows that evolve along their unstable directions become fully turbulent. The solution approached by a threshold perturbation could depend upon the nature of the perturbation. Surprisingly, the positive eigenvalue that corresponds to one family of solutions decreases in magnitude with increasing Re, with the rate of decrease given by Re^{α} with $\alpha \approx -0.46$.

1 Introduction

1.1 Transition to Turbulence

The classical problem of transition to turbulence in fluids has not been fully solved in spite of attempts spread over more than a century. Transition to turbulence manifests itself in a simple and compelling way in experiments. For instance, in the pipe flow experiment of Reynolds (see [1]), a dye injected at the mouth of the pipe extended in "a beautiful straight line through the tube" at low velocities or low Reynolds numbers (Re). The line would shift about at higher velocities, and at yet higher velocities the color band would mix up with the surrounding fluid all at once at some point down the tube.

A wealth of evidence shows that the incompressible Navier–Stokes equation gives a good description of fluid turbulence. Therefore one ought to be able to understand the transition to turbulence using solutions of the Navier–Stokes equation. However, the nature of the solutions of the Navier–Stokes equation is poorly understood. Thus the problem of transition to turbulence is fascinating both physically and mathematically.

The focus of this paper is on plane Couette flow. In plane Couette flow, the fluid is driven by two plane parallel walls. If the fluid is driven hard enough, the flow becomes turbulent. Such wall driven turbulence occurs in many practical situations such as near the surface of moving vehicles and is technologically important.

The two parallel walls are assumed to be at $y = \pm 1$. The walls move in the x or streamwise direction with velocities equal to ± 1. The z direction is called the spanwise direction. The Reynolds number is a dimensionless constant obtained as $Re = UL/\nu$, where U is half the difference of the wall velocities, L is half the separation between the walls, and ν is the viscosity of the fluid. The velocity of the fluid is denoted by $\mathbf{u} = (u, v, w)$, where u, v, w are the streamwise, wall-normal, and spanwise components.

For the laminar solution, $v = w = 0$ and $u = y$. The laminar solution is linearly stable for all Re. As shown by Kreiss et al. [7], perturbations to the laminar solution that are bounded in amplitude by $O(Re^{-21/4})$ decay back to the laminar solution. However, in experiments and in computations, turbulent spots are observed around $Re = 360$ [2]. The transition to turbulence in such experiments must surely be because of the finite amplitude of the disturbances. By a threshold disturbance, we refer to a disturbance that would lead to transition if it were slightly amplified but which would relaminarize if slightly attenuated. The concept of the threshold for transition to turbulence was highlighted by Trefethen and others [16]. The amplitude of the threshold disturbance depends upon the type of the disturbance. It is believed to scale with Re at a rate given by Re^{α} for some $\alpha <= -1$.

Our main purpose is to explain how certain finite amplitude disturbances of the laminar solution lead to turbulence. The dynamical picture that will be developed in this paper is illustrated in Fig. 1. Historically, the laminar solution itself has been the focus of attempts to understand mechanisms for transition. Our focus however will be on a different solution that is represented as an empty oval in Fig. 1.

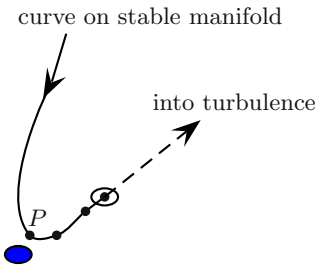

Fig. 1. Schematic sketch of the dynamical picture of transition to turbulence that is developed in this paper. The *solid oval* stands for the laminar solution, and the *empty oval* stands for a steady or traveling wave solution

Solutions that could correspond to the empty oval in Fig. 1 will be called lower-branch solutions [11, 19]. A solution at a certain value of Re can be continued by increasing a carefully chosen parameter. When this parameter is increased, Re first decreases and begins to increase after a bifurcation point and we end up with an "upper branch solution" at the original value of Re. The fact that a continuation procedure can lead to an upper-branch solution appears to have no significance for the dynamics at a fixed value of Re, however.

Depending upon the type of disturbance, the lower-branch solution could either be a steady solution or a traveling wave. Those solutions are not laminar in nature. Neither are they fully turbulent even at high Re. Unlike the laminar solution, these solutions are linearly unstable. The lower-branch solutions remain at an $O(1)$ distance from the laminar solution, while the threshold amplitudes decrease with Re as indicated already. Therefore the threshold disturbances are too tiny to perturb the laminar solution directly onto a lower-branch solution. We will show, however, that some threshold disturbances perturb the laminar solution to a point on the stable manifold of a lower-branch solution (point P in Fig. 1). A slightly larger disturbance brings the flow close to the lower-branch solution, after which the flow follows a branch of its unstable manifold and becomes fully turbulent.

For certain types of disturbances, the perturbed laminar solution does not approach a lower branch solution. Thus the dynamical picture of Fig. 1 is not valid for those disturbances. Instead it flows towards an *edge state* [15]. We give a brief discussion of the nature of the edge states in Sect. 4.

1.2 Connections to Earlier Research

The dynamical picture presented in Fig. 1 is related directly and indirectly to much earlier research. Basic results from hydrodynamic stability show that some eigenmodes that correspond to the least stable eigenvalue of the linearization around the laminar solution do not depend upon the spanwise or z direction. This may lead one to expect that disturbances that trigger transition to turbulence are 2-dimensional. That expectation is not correct, however. As shown by Orszag and Kells [13], spanwise variation is an essential feature of disturbances that trigger transition to turbulence. Accordingly, all the disturbances considered in this paper are 3-dimensional.

Kreiss et al. [7] and Lundbladh et al. [9] investigated disturbances that are non-normal pseudomodes of the linearization of the laminar solution. Since the laminar solution is linearly stable, a slight perturbation along an eigenmode will simply decay back to the laminar solution at a predictable rate. The pseudomodes are chosen to maximize transient growth of the solution of the linearized equation, which is a consequence of the non-normality of the linearization. Such disturbances lead to transition with quite small amplitudes and will be considered again in this paper. It must be noted, however, that any consideration based on the linearization alone can only be valid in a small

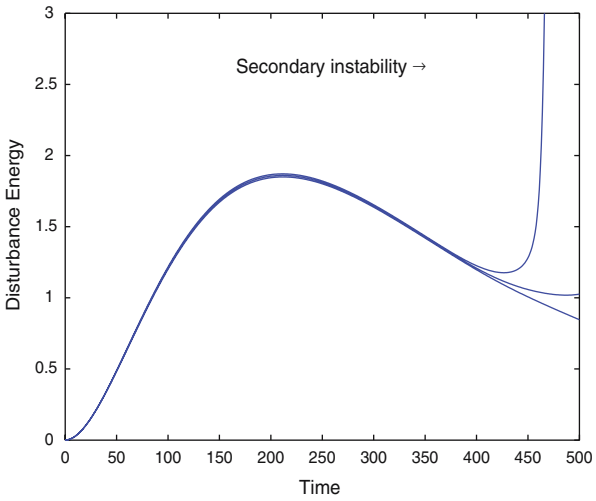

Fig. 2. The plot above shows the secondary instability in a transition computation at $Re = 2{,}000$

region around the laminar solution. The dynamics of transition to turbulence, as sketched in Fig. 1, involves an approach towards a lower-branch solution that lies at an $O(1)$ distance from the laminar solution. It is therefore necessary to work with the fully nonlinear Navier–Stokes equation to explicate the dynamics of transition to turbulence.

Figure 2 shows the variation of the disturbance energy with time for a disturbance that leads to transition. We observe that the disturbance energy increases smoothly initially and is then followed by a spike. The spike is in turn followed by turbulence. The spike corresponds to a secondary instability, as noted by Kreiss et al. [7]. In fact, the so-called secondary instability is just the linear instability of a lower-branch solution as will become clear.

Partly motivated by the secondary instability, there was a search for nonlinear steady solutions related to transition as reviewed in [3]. Early success in this effort was due to Nagata [11, 12] who computed steady solutions of plane Couette flow in the interval $125 \leq Re \leq 300$. Waleffe [18, 19, 20] introduced a more flexible method for computing such solutions, and like Nagata, argued that such solutions could be related to transition to turbulence. The numerical method we use was introduced in [17]. It uses a combination of Krylov space methods and the locally optimally constrained hook step to achieve far better resolution as shown by [4, 17] and this paper.

The computations in [7, 9] imply that threshold amplitudes scale as Re^{α} for $\alpha < -1$. The value of α appears to depend upon the type of perturbation. Our focus is not on determining the scaling of the threshold amplitudes. Nevertheless, we will discuss numerical difficulties that beset determination of threshold amplitudes.

Measuring threshold amplitudes poses experimental challenges as well and it is not always clear from experiments if the thresholds have a simple power scaling with Re. One difficulty is that the turbulent states can be short lived. Schmiegel and Eckhardt [14] have connected the lifetime of turbulence to the possibility that turbulent dynamics in the transition regime is characterized by a chaotic repeller and not a chaotic attractor.

1.3 Connections to Recent Research

Wang et al. [21] have taken steps towards an asymptotic theory of the lower branch solutions and carried their computation beyond $Re = 50,000$. They connect the asymptotics to scalings of the threshold for transition to turbulence. The lower branch states occur as solutions to equations that use periodic boundary conditions. Because such boundary conditions cannot be realized in laboratory setups, the solutions are best thought of as waves. Thus it is pertinent to consider their stability with respect to subharmonic disturbances as in [21]. That paper also suggests that lower branch solutions might be of use for control. A somewhat different suggestion related to control can be found in [5].

Not all disturbances follow the dynamical picture of Fig. 1 as already noted. For the third type of disturbance considered in Sect. 4, the laminar solution perturbed by the threshold disturbance evolves towards a state that looks almost like an invariant object of the underlying differential equation. Those objects have been termed edge states by Schnieder et al. [15]. Lagha et al. [8] make the important point that the dynamical picture of Fig. 1 can be valid for typical disturbances only if the lower-branch solution has a single unstable eigenvalue.

Near the threshold for the third type of disturbance, it appears as if the disturbed state evolves and approaches a traveling wave. Indeed, a crude or under-resolved computation could easily mistake that appearance for a true solution. When we attempted to refine that near-solution using the numerical method reviewed in Sect. 3, the numerical method converged to a traveling wave solution. However, that traveling wave has two unstable eigenvalues and the flow near the threshold does not come as close to that traveling wave as the dynamical picture of Fig. 1 would require.

Visualizing the dynamics in state space is fundamental to the approach to transition to turbulence sketched in this paper and in the articles discussed above. Yet there has so far been no way to obtain revealing visualizations of state space dynamics. Gibson et al. [4] have recently produced revealing visualizations of the state space of turbulent flows. For instance, one of their figures shows a messy-looking turbulent trajectory cleanly trapped by the unstable manifolds of certain equilibrium solutions.

Section 2 reviews some basic aspects of plane Couette flow. The numerical method used to flesh out the dynamical picture of Fig. 1 is given in Sect. 3. In

Sect. 4, we consider three different types of disturbances. The lower-branch solutions (empty oval of Fig. 1) that correspond to the first two types are steady solutions. For a given Re, the solutions that correspond to these two types are identical modulo certain symmetries of plane Couette flow. In Sect. 5, we consider some qualitative aspects of the solutions reported in Sect. 4. A surprising finding is that these these solutions are less unstable for larger Re. The top eigenvalue of these solutions is real and positive. For one family of solutions, the top eigenvalue appears to decrease at the rate Re^{α} for $\alpha \approx -0.46$.

In the concluding Sect. 6, we give additional context for this paper from two points of view. The first point of view is mainly computational and has to do with reduced dimension methods. In this paper, we have taken care to use adequate spatial resolution to ensure that the computed solutions are true solutions of the Navier–Stokes equation. We recognize, however, that resolving all scales may prove computationally infeasible in some practical situations. We argue that transition to turbulence computations can be useful in gaging the possibilities and limitations of methods that do not resolve all scales. Secondly, we briefly discuss the connection of transition computations with transition experiments.

2 Some Aspects of Plane Couette Flow

The Navier–Stokes equation $\partial\mathbf{u}/\partial t + (\mathbf{u}.\nabla)\mathbf{u} = -(1/\rho)\nabla p + (1/Re)\triangle\mathbf{u}$ describes the motion of incompressible fluids. The velocity field $\mathbf{u}$ satisfies the incompressible constraint $\nabla.\mathbf{u} = 0$. For plane Couette flow the boundary conditions are $\mathbf{u} = (\pm 1, 0, 0)$ at the walls, which are at $y = \pm 1$. To render the computational domain finite, we impose periodic boundary conditions in the x and z directions, with periods $2\pi\Lambda_x$ and $2\pi\Lambda_z$, respectively. To enable comparison with [9], we use $\Lambda_x = 1.0$ and $\Lambda_z = 0.5$ throughout this paper.

Certain basic quantities are useful for forming a general idea of the nature of a velocity field of plane Couette flow. The first of these is the rate of energy dissipation per unit volume for plane Couette flow, which is given by

$$D = \frac{1}{8\pi^2\Lambda_x\Lambda_z}\int_0^{2\pi\Lambda_z}\int_{-1}^{+1}\int_0^{2\pi\Lambda_x} |\nabla u|^2 + |\nabla v|^2 + |\nabla w|^2 \; dx\, dy\, dz. \qquad (1)$$

The rate of energy input per unit volume is given by

$$I = \frac{1}{8\pi^2\Lambda_x\Lambda_z}\int_0^{2\pi\Lambda_x}\int_0^{2\pi\Lambda_z} \frac{\partial u}{\partial y}\Big|_{y=1} + \frac{\partial u}{\partial y}\Big|_{y=-1} dx\, dz. \qquad (2)$$

For the laminar solution $(u, v, w) = (y, 0, 0)$, both D and I are normalized to evaluate to 1. Expressions such as (1) and (2) are derived using formal manipulations. The derivations would be mathematically valid if the velocity field $\mathbf{u}$ were assumed to be sufficiently smooth. Although such smoothness

properties of solutions of the Navier–Stokes are yet to be proved, numerical solutions possess the requisite smoothness. Even solutions in the turbulent regime appear to be real analytic in the time and space variables, which is why spectral methods have been so successful in turbulence computations.

In the long run, on physical grounds, we expect the time averages of D and I to be equal because the energy dissipated through viscosity must be input at the walls. For steady solutions and traveling waves, the values of D and I must be equal.

Another useful quantity is the disturbance energy. The disturbance energy of (u, v, w) is obtained by integrating $(u-y)^2+v^2+w^2$ over the computational box. This quantity has already been used in Fig. 2. The disturbance energy is a measure of the distance from the laminar solution.

Two discrete symmetries of the Navier–Stokes equation for plane Couette flow will enter the discussion later. The shift-reflection transformation of the velocity field is given by

$$S_1\mathbf{u} = \begin{pmatrix} u \\ v \\ -w \end{pmatrix} \left(x + \pi\Lambda_x, y, -z \right), \tag{3}$$

and the shift-rotation transformation of the velocity field is given by

$$S_2\mathbf{u} = \begin{pmatrix} -u \\ -v \\ w \end{pmatrix} \left(-x + \pi\Lambda_x, -y, z + \pi\Lambda_z \right). \tag{4}$$

Plane Couette flow is unchanged under both these transformations. Thus if a single velocity field along a trajectory of plane Couette flow satisfies either symmetry, all points along the trajectory must have the same symmetry. However, velocity fields that lie on the stable and unstable manifolds of symmetric periodic or relative periodic solutions need not be symmetric.

3 Numerical Method

The Navier–Stokes equation in the standard form given in Sect. 2 cannot be viewed as a dynamical system because the velocity field $\mathbf{u}$ must satisfy the incompressibility condition and because there is no equation for evolving the pressure p. It can be recast as a dynamical system, however, by using the y components of $\mathbf{u}$ and $\nabla \times \mathbf{u}$, which is the vorticity field. If the resulting system is discretized in space using $M + 1$ Chebyshev points in the y direction, and $2L$ and $2N$ Fourier points in the x and z directions, respectively, the number of degrees of freedom of the spatially discretized system is given by

$$2(M-1) + (2M-4)((2N-1)(2L-1)-1) \tag{1}$$

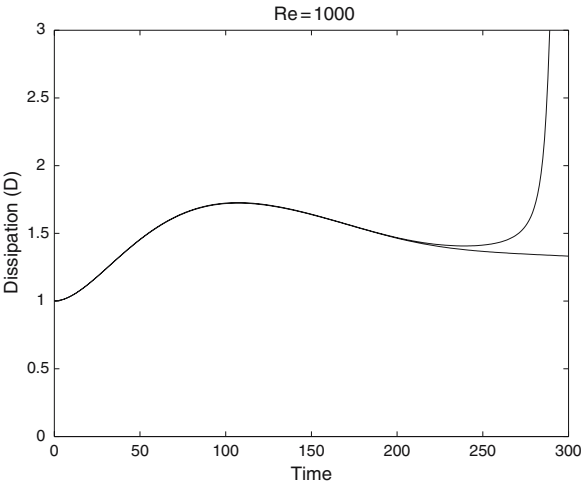

Fig. 3. The plot above shows the variation of D defined by (1) for a disturbance slightly above the threshold and for a disturbance slightly below the threshold

as shown in [17]. We do not use a truncation strategy to discard modes and we employ dealiasing in the directions parallel to the wall.

Given a form of the disturbance P, the threshold for transition is obtained by integrating the disturbed velocity $(y, 0, 0) + \epsilon P$ in time for different ϵ [7]. If ϵ is greater than the threshold value, the flow will spike and become turbulent as evident from Figs. 2 and 3. If ϵ is below the threshold value, the flow will relaminarize. As indicated by Figs. 2 and 3, we may graph either disturbance energy or D to examine a value of ϵ. We may also graph I, which is defined by (2), against time.

The accurate determination of thresholds is beset by numerical difficulties. To begin with, suppose that we are able to integrate the Navier–Stokes equation for plane Couette flow exactly. Then as implied by the dynamical picture in Fig. 1, a disturbance of the laminar solution that is on the threshold will fall into a lower-branch solution, and it will take infinite time to do so. However, computations for determining the threshold, such as that shown in Fig. 2, can only be over a finite interval of time. Thus the finiteness of the time of integration is a source of error in determining thresholds. Two other sources of error are spatial discretization and time discretization.

An accurate determination of the threshold will need to estimate and balance these three sources of error carefully. In our computations, we determine the thresholds with only about two digits of accuracy. That modest level of accuracy is sufficient for our purposes. In Tables 1 and 3, the thresholds are reported using disturbance energy per unit volume.

Once the threshold has been determined, we need to compute a steady solution or a traveling wave to complete the dynamical picture of Fig. 1. The

Table 1. Data for disturbances of the form (1) with unsymmetric noise and for steady solutions that correspond to the empty oval in Fig. 1

Label	Re	D/I	λ_{max}	Re_τ	T	Threshold
$B1$	500	1.3920	0.04326	53	150	$2.46e-4$
$B2$	1,000	1.3486	0.03294	73	300	$5.73e-5$
$B3$	2,000	1.3285	0.02413	103	500	$1.36e-5$
$B4$	4,000	1.3210	0.01732	145	1,000	$3.30e-6$

The steady solutions are labeled $B1$ through $B4$. D and I, which are defined by (1) and (2), correspond to those steady solutions. The next two columns give the eigenvalue with the maximum real part and the frictional Reynolds number for those solutions. T is the time interval used to determine the threshold disturbance and the threshold is reported using disturbance energy per unit volume

initial guess for that lower-branch solution is produced by perturbing the laminar solution by adding the numerically determined threshold disturbance and integrating the perturbed point over the time interval used for determining the threshold (this time interval is 500 in Fig. 2 and 300 in Fig. 3).

That initial guess is fed into the method described in [17] to find a lower-branch solution with good numerical accuracy. That method finds solutions by solving Newton's equations, but the equations are set up and solved in a non-standard way. Suppose that the spatially discretized equation for plane Couette flow is written as $\dot{x} = f(x)$, where the dimension of x is given by (1). To find a steady solution, for instance, it is natural to solve $f(x) = 0$ after supplementing that equation by some conditions that correspond to the symmetries (3) and (4). However that is not the way we proceed. We solve for a fixed point of the time t map $x(t; x_0)$, for a fixed value of t, after accounting for the symmetries. The Newton equations are solved using GMRES. The method does not always compute the full Newton step, however. Instead, the method finds the ideal trust region step within a Krylov subspace as described in [17].

This method can easily handle more than 10^5 degrees of freedom, and thus makes it possible to carry out calculations with good spatial resolution. The reason for setting up the Newton equations in the peculiar way described in the previous paragraph has to do with the convergence properties of GMRES. The matrix that arises in solving the Newton equations approximately has the form $I - \partial x(t; x_0)/\partial x_0$, where I is the identity. Because of viscous damping of high wavenumbers, many of the eigenvalues of that matrix will be close to 1, thus facilitating convergence of GMRES. We may expect the convergence to deteriorate as Re increases, because viscous damping of high wavenumbers is no longer so pronounced, and that is indeed the case. Nevertheless, we were able to go up to $Re = 4{,}000$, and we believe that even higher values of Re can be reached.